Journal for ImmunoTherapy of Cancer

Systematic evaluation of neoepitope predictions challenges clinically observed T-cell responses and their impact on immune evasion

Badeel Kh Q Zaghla ,[1] Zuhal Safyürek ,[1] Daniela Gröger,[1] Shima Mecklenbräuker,[1] Nina-Sophie Lingstädt,[1] Oliver Popp,[2] Johanna Spengler,[1] Mohamed Haji,[2] Meagan Montesion,[3] Lee A Albacker,[3] Philipp Mertins,[2,4] Martin G Klatt [1,5]

Abstract Peptide presentation on human leukocyte antigens (HLAs) is essential for initiating T-cell responses and all consequences of this presentation including anticancer immunity or immune escape. Many studies have relied on in silico prediction tools rather than biological measurement of HLA presentation to study these effects. To better assess the frequency and consequences of neoantigen presentation, we overexpressed 125 combinations of full-length neoantigens and one HLA class I allele to experimentally validate presentation of mutated and non-mutated HLA ligands through HLA ligand isolation followed by tandem mass spectrometry. A successful presentation was observed only in 22% of predicted cases with strong implications on previously described downstream effects. For example, the association of HLA loss of heterozygosity with predicted neoepitopes was challenged for 58% (73/125) of combinations. Furthermore, when testing 51 sequences used for personalized messenger RNA neoepitope vaccines, we observed that clinical responses were independent of the presentation status of the neoepitopes. Even a presumably neoepitope-specific and strongly expanded T cell receptor clone from a neoantigen vaccination study could not be linked to a successfully presented neoepitope. Overall, these data highlight the importance of validating the presentation of neoepitopes to fully understand our interpretation of clinical mutation-specific responses and their related effects, including immune evasion.

To cite: Zaghla BKQ, Safyürek Z, Gröger D, *et al*. Systematic evaluation of neoepitope predictions challenges clinically observed T-cell responses and their impact on immune evasion. *Journal for ImmunoTherapy of Cancer* 2026;**11**:e013271. doi:10.1136/jitc-2025-013271

► Additional supplemental material is published online only. To view, please visit the journal online (https://doi.org/10.1136/jitc-2025-013271).

Accepted 19 December 2025

For numbered affiliations see end of article.

Correspondence to
Dr Martin G Klatt;
martin.klatt@charite.de

INTRODUCTION

T cell-based immunotherapies are a promising approach for the treatment of metastatic cancer that target tumor-specific or tumor-associated antigens presented on the surface of cancer cells.[1 2] These therapies rely on the recognition of small peptides derived from intracellular proteins, which are processed by the proteasome and presented on human leukocyte antigen (HLA) class I molecules. Many studies investigate the biological consequences of neoepitope presentation in the context of T cell-based therapies, which are then used to predict outcome after therapy with immune checkpoint blockade therapy or associated events of immune evasion.[3–5] However, the neoepitopes these studies are based on are regularly only predicted and not experimentally confirmed. Similarly, personalized neoepitope vaccine studies use prediction algorithms to define the composition of their vaccine [6–8] and clinical effects following T-cell responses like immune evasion by HLA loss of heterozygosity (HLA-LOH) are regularly explored by defining neoepitopes through prediction algorithms.[4 5]

But, despite their utility for hypothesis generation, current prediction algorithms remain suboptimal and carry the risk of creating both false positive and false negative results.[9] The gold standard to reduce the risk of false positive results is therefore to prove presentation of HLA ligands through the isolation of HLA complexes and their presenting peptides with subsequent mass spectrometry (MS) analysis.[10 11] To investigate the reliability of these prediction tools and to improve our understanding of neoepitope presentation and their biological implications, we systematically analyzed the presentation status of 125 predicted public and 51 private neoepitopes. First, we optimized co-transfection experiments of one full-length neoantigen and one HLA-I allele followed by peptide:HLA (pHLA) isolation and MS analysis to minimize the risk of false negative results and to define high confidence neoepitopes.[12 13] Even under these favorable experimental conditions, sufficient pHLA-I presentation was confirmed in only 22% of 176 tested combinations with highest relevance for the interpretation of clinical data on immune evasion, monitoring of neoepitope T-cell responses and vaccine design.

RESULTS

A co-transfection-based overexpression system enables robust neoepitope profiling

To explore the correlation of neoepitopes, immune responses and their biological implications, we first defined which of the investigated mutations carry the potential to be presented on a specific HLA allele. In detail, we first established our pipeline of co-transfecting a monkey fibroblast cell line (COS-7) that expresses antigen processing genes highly homologous to humans with messenger RNA (mRNA) from both a mutated antigen and one HLA-I allele as described before (figure 1A).[12 13] We confirmed transfection efficiency of at least 90% for all evaluable HLA-I alleles (online supplemental fig S1A,S1B) and combined this system with our highly sensitive immunopeptidomics pipeline.[14 15] This includes the immunoprecipitation of pHLA complexes, biochemical isolation of the bound peptides and subsequent tandem MS which identifies the amino acid sequences of the presented peptides. Using this approach, we detected the well-characterized KRAS G12V shared (or 'public') neoantigen in the context of HLA-A*03:01 in as few as 500,000 cells using untargeted MS (figure 1B). By using 10 million COS-7 cells, that is, 20 times as many cells as needed for detection in our pipeline, for all following experiments, we aimed to minimize the risk of false negative results. Additionally, we confirmed for another well-studied neoantigen:HLA-I combination (KRAS G12V:HLA-A*02:01) that non-detection was neither due to insufficient transfection of the target antigen nor the HLA allele (online supplemental fig S1C,S1D). Additionally, all transfected HLA alleles led to the robust presentation of hundreds of HLA ligands derived from endogenous COS-7 proteins, with an average of 594 ligands, as determined by our immunopeptidome experiments (online supplemental fig S2), (online supplemental data S1). This robust presentation of HLA ligands on the transfected HLA allele serves as another validation that transfections were successful if no allele-specific antibody was available to confirm its surface expression. Additionally, we quantified the number of neoepitopes presented on the cell surface for the combination of HLA-A*11:01 and KRAS G12D using MS to be 9,970 molecules per cell. These data underline the very effective presentation machinery of COS-7 cells, which together with their robustness during the transfection process provided the rationale to use this cell line.

Immunopeptidome analysis of co-transfections highlights strong discrepancy between predicted and experimentally validated presentation of HLA ligands

Having established an experimental set-up that has the capacity to display potential peptides from a given antigen in the context of one HLA allele, we wanted to investigate which fraction of predicted HLA ligands can be validated experimentally and how these results correlate with biological effects, like HLA-LOH. Thus, we examined 127 neoantigen/HLA-I combinations for which at least 30 HLA-LOH events were reported in a cohort of 83,644 patients with cancer.[4] 75% of these combinations were associated with a significant loss of the HLA allele that was predicted to present a public neoepitope from the investigated neoantigen. Of these 127 pairs, 2 combinations (TP53 R175H/HLA-A*02:01 and TP53 Y220C/HLA-A*02:01) were already tested with full-length antigens in the COS-7 system,[16 17] leaving 125 untested.

Notably, on average, only 9.5% of mutated or unmutated HLA ligands predicted to be presented on the transfected HLA allele and derived from the transfected full-length antigens were experimentally validated (figure 1C). While some combinations, such as KRAS with HLA-A*02:01, HLA-A*11:01, or HLA-C*08:02, had higher accuracy compared with other alleles, no HLA allele consistently showed better results demonstrating an allele-independent discrepancy between predicted and identified HLA ligands (online supplemental fig S3A). Although the prediction score had no significant effect on presentation in the mutated peptide group (figure 1D–F), non-mutated peptides had a highly significant better chance of getting presented if they achieved better prediction scores (figure 1G–I).

In consequence, only 23.1% of the 125 combinations resulted in successful presentation of a neoepitope independently if HLA-LOH was significantly associated with these pairs or not (figure 2A, online supplemental fig S3B, (online supplemental table S1). In retrospect, these data match previous reports that confirmed neoepitope presentation for 23.6% of neoantigen:HLA pairs after we filtered these datasets for combinations that were also predicted to present neoepitopes associated with HLA-LOH (online supplemental fig S3B).[18 19] Still, nine previously published KRAS neoepitopes from seven combinations (G12D in HLA-A*11:01, G12D in HLA-C*08:02 as well as G12V, G12C, G12A, G12S, in HLA-A*11:01, and G12R in HLA-A*03:01),[18 19] were successfully validated. Additionally, 24 undescribed public neoepitopes across 11 HLA alleles from 8 different neoantigens were identified, including public neoantigens evolving from resistance-associated mutations (*ESR1* D538G and *EGFR1* T790M) (figure 2A, (online supplemental fig S4,S5) and online supplemental table S1). Since peptide processing and presentation could still vary between a cell line of monkey and human origin, we repeated a subset of co-transfection with K562 cells. Successful co-transfection of K562 cells was confirmed for one representative allele (HLA-A*02:01, online supplemental fig S6A-C) and five positive as well as nine negative combinations were tested. All positive and negative results aligned perfectly with our previous results in COS-7 cells. Of note, five negative combinations were also tested after treating K562 cells with interferon (IFN)-γ which did not alter the observed results (online supplemental table S2). However, it cannot be ruled out that some public neoepitopes can only be successfully processed and presented in the presence of the immunoproteasome.

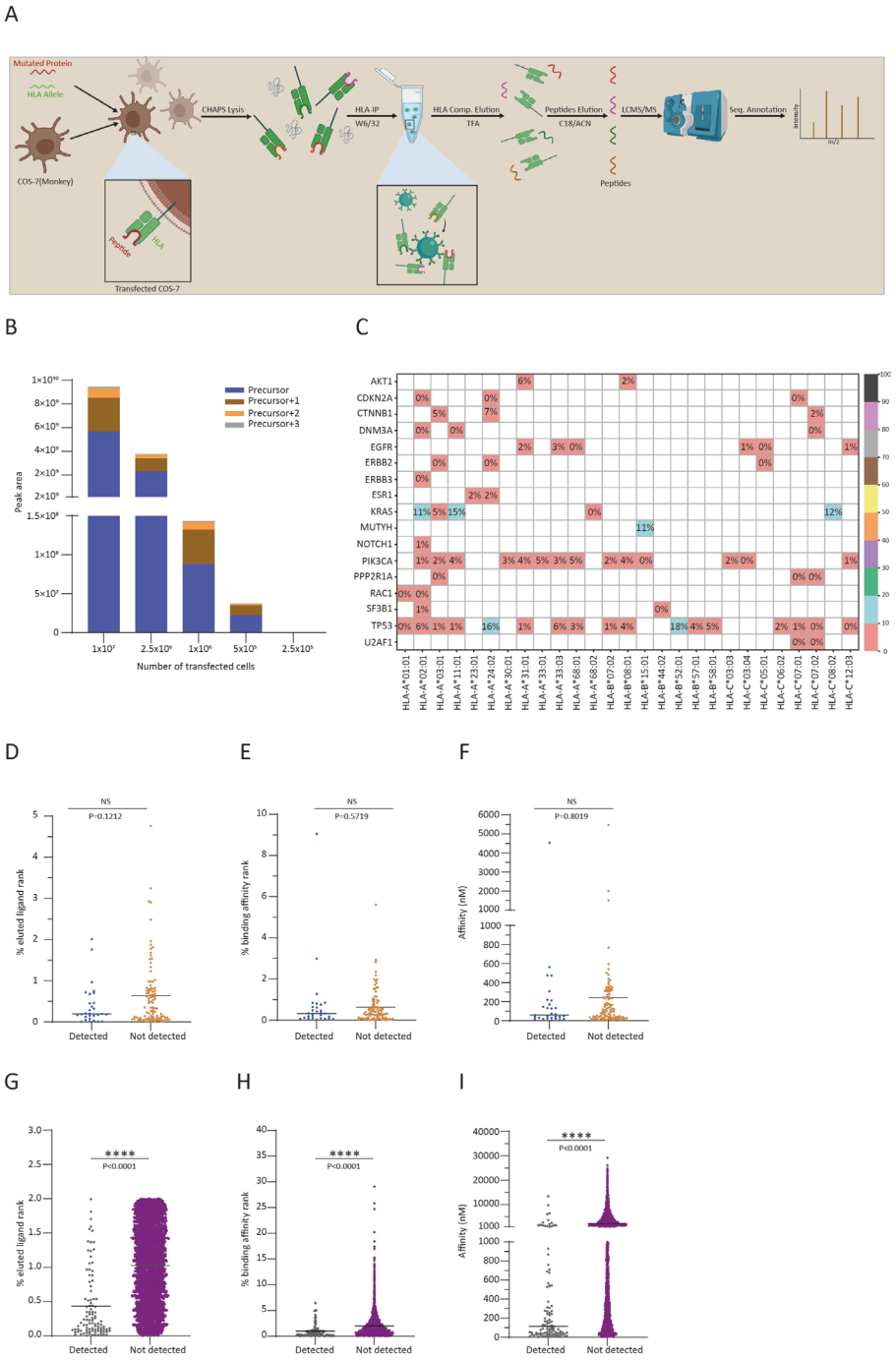

Figure 1 Workflow and characteristics of co-transfection immunopeptidome experiments. (A) Experimental procedure for the identification of HLA ligands from selected antigens using a co-transfection strategy followed by biochemical HLA ligand isolation and analyses via tandem mass spectrometry. (B) Relative abundance of the KRAS G12V-derived public neoantigen presented by HLA-A*11:01 in various cell numbers, quantified using Skyline. Precursors refer to the full peptide before fragmentation and "+1", "+2", "+3" to isotopic variants of the same peptide. (C) Heatmap showing the fraction of experimentally detected (mutated and non-mutated) peptides relative to predicted HLA ligands for each protein/HLA combination. For this analysis, all data from one protein (eg, KRAS) independent of the different mutations (eg, G12V, G12D) were pooled. For each protein of interest, the number of detected peptides was divided by the number of predicted binders that are derived from the whole protein sequence including mutated and unmutated peptides as defined by NetMHCpan 4.1 (EL rank ≤2). The resulting fractions are depicted as percentages which are color-coded based on higher or lower detected fractions. (D–I) Differences in prediction scores for detected and non-detected (=only predicted) HLA ligands (same peptides as predicted in C). All scores were obtained by NetMHCpan 4.1. (D–F) Compares prediction scores for public neoepitopes, whereas (G–I) compares scores for unmutated peptide sequences. (D,G) EL rank refers to a relative scoring trained on immunopeptidome datasets, whereas BA rank in (E,H) is a relative scoring matrix based on affinity measurements between peptides and HLA complexes. In (F,I)* used absolute binding affinity predictions (IC50 in nM) as defined by NetMHCpan 4.1. Unpaired Student's t-test was performed for comparisons. *p<0.05, ****p<0.0001. BA, binding affinity; EL, eluted ligand; HLA, human leukocyte antigen; NS, not significant.

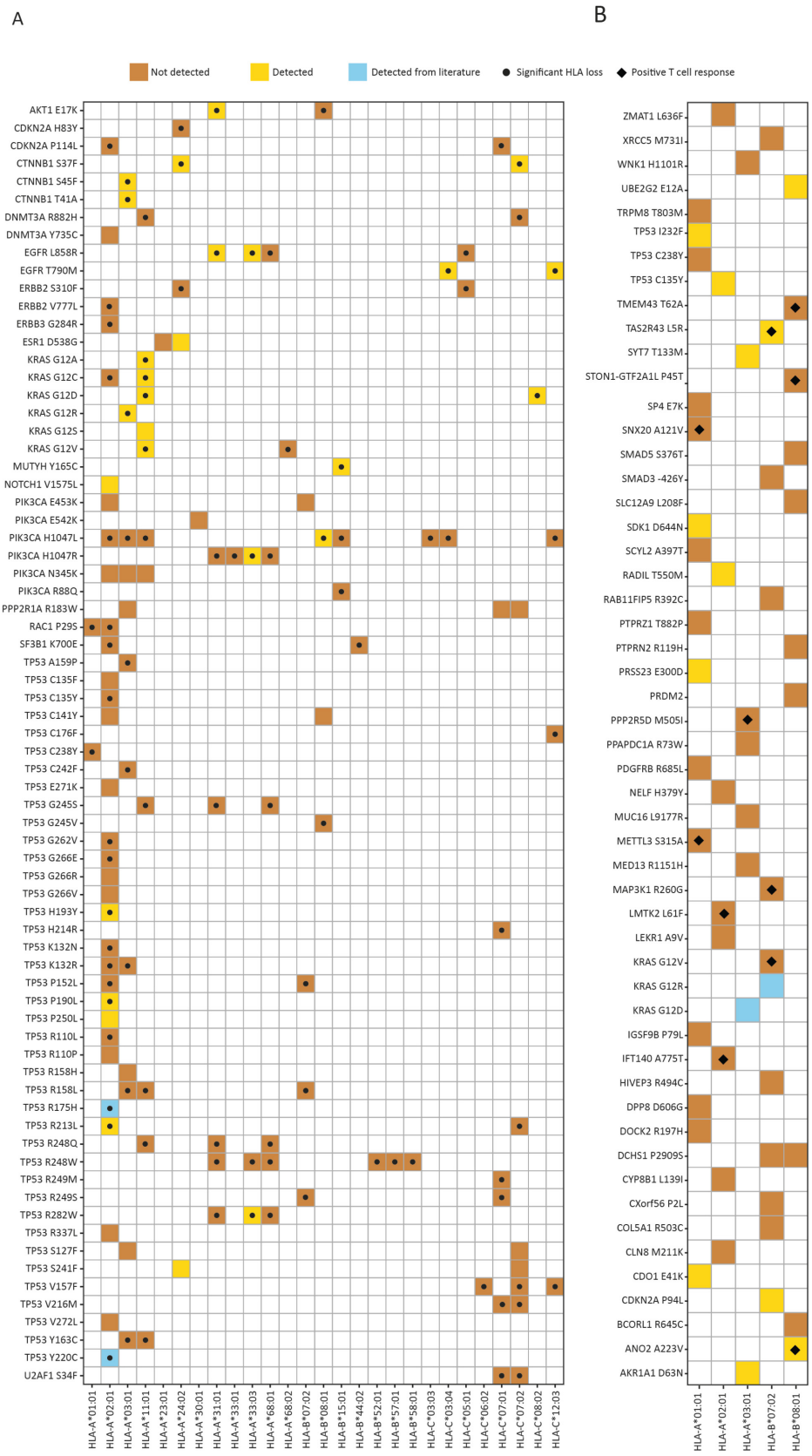

Figure 2 Analysis of HLA/neoantigen combinations, HLA-LOH, and clinical T-cell responses. (A–B)* showing screened public neoantigen–HLA combinations. Brown squares indicate undetected neoantigen-HLA pairs. Yellow squares represent detected neoantigen-HLA pairs. Blue squares denote neoantigens that were previously detected from the literature. Squares with centered dots indicate reports of significant HLA loss. Squares with polygon indicate positive clinical T-cell responses in patients who received personalized neoantigen-based mRNA cancer vaccine. HLA, human leukocyte antigen; LOH, loss of heterozygosity; mRNA, messenger RNA.

Still, these data highlight the limited capacity of prediction algorithms to define public neoepitopes on a larger scale. Thus, downstream analyses associated with the predictions like immune evasion through HLA-LOH should ideally be complemented by immunopeptidome analyses to better understand the links between HLA-LOH and presentation of public neoepitopes.

Individual mRNA neoepitope vaccine responses show no correlation with presentation status of mutated HLA ligands

Private neoepitopes resulting from passenger mutations are frequently used in clinical and preclinical studies for the generation of personalized neoantigen vaccines.[6–8] Because these vaccines need to be designed in a time-efficient manner, they rely almost exclusively on prediction algorithms and thus presentation of these private neoepitopes has not been evaluated systematically. We therefore expanded our co-transfection experiments to include 15-mer minigenes that had been used as mRNA vaccines in a recent phase I clinical trial which investigated the effect of an adjuvant neoantigen vaccine in combination with immune checkpoint blockade and standard chemotherapy in pancreatic duct adenocarcinoma.[7] We selected mutations that were predicted to be presented in the context of the highly prevalent and well-characterized HLA-A*01:01, HLA-A*02:01, HLA-A*03:01, HLA-B*07:02, and HLA-B*08:01 alleles to improve comparability. Overall, minigenes from 14/16 patients were analyzed in this study. This selection yielded 53 combinations for which clinical T-cell monitoring data were available, allowing us to correlate presentation status of the investigated neoantigens with immunogenicity. Of these 53 pairs, 2 combinations (KRAS G12D/HLA-A*03:01 and KRAS G12R/HLA-B*07:02) were previously validated by other immunopeptidome studies, leaving 51 untested.

We identified 12 private neoepitopes across 5 HLA alleles from 51 combinations which resembled perfectly the rate of successful presentations (23.5%) from our previous experiments (figure 2B, online supplemental fig S4, S5 and table S1). Consistent with our results studying putative public neoantigens, presentation of private neopeptides was significantly associated with better binding prediction scores (online supplemental fig S3C-E). Surprisingly, our analysis found no significant correlation between neoepitope presentation and reported T-cell responses (online supplemental fig S3F). Only 2 of the 12 detected neoepitopes corresponded with positive immune responses reported in clinical trials, while the remaining 10 did not. Thus, the positive rate for T-cell responses was 16.7% (2/12) in the group of presented neoepitopes and 23% (9/39) in the group of non-presented neoepitopes. Additionally, over 80% of observed T-cell responses (9/11) could not be linked to successful presentation of these neoepitopes (figure 3A). For example, neoepitopes derived from the co-transfection of B*07:02/KRAS G12V against which a positive T-cell response was reported, were neither detected in our study nor in two previous immunopeptidome studies that explored public neoepitopes derived from this combination.[17 18] Although it might be possible that these neoepitopes are recognized by T cells at a level of just a few molecules per cell, the undetectability in a strong overexpression system questions the presentation in regular tumor tissue and thus the possibility to trigger these T-cell responses.

Additionally, polyclonal T-cell responses were reported and presumably mutation-specific T-cell receptors isolated against the PLXNB3 Q1897K minigene in the context of HLA-A*32:01. Nevertheless, our pipeline did not detect any HLA-A*32-restricted HLA ligands derived from this minigene, whereas a peptide from the CMV-pp65 antigen with known positive T-cell reactivity was presented on this allele as a positive control (figure 3B).

To further investigate if the positive T-cell response observed against PLXNB3 Q1897K might be mediated by a human cytomegalovirus (HCMV)-specific A*32 restricted T-cell response, we stimulated T cells from HLA-A*32:01 positive healthy blood donors with the validated pp65-derived peptide loaded onto autologous dendritic cells (DCs). Then, HCMV-primed T cells were incubated with DCs either loaded with HCMV pp65 or the mutated PLXNB3 peptide. We used intracellular IFN-γ staining as a readout and confirmed similar activation levels of the primed T cells if exposed to the pp65 or the PLXNB3 peptide suggesting that the reported T-cell response in the clinical trial might have been mediated by a HCMV-specific T cell receptor (TCR) clone or any other cross-reactive TCR (figure 3C and D).

Altogether, these data highlight that T-cell responses against individual neoepitope should be matched with immunopeptidome analysis to be able to deconvolute truly neoepitope-specific T-cell responses in contrast to cross-reactivities facilitated through in vitro assays.

DISCUSSION

Here, we demonstrate a significant discrepancy between predicted and experimentally validated neoepitopes as well as their reported recognition by T cells. Using full-length neoantigens and single HLA-I alleles, we minimized biases through antigen and HLA allele competition, processing as well as expression if multiple minigenes are combined in single vectors.[18] Still, only 22% of combinations resulted in successful presentation of the predicted neoepitopes, which nevertheless led to the definition of 24 previously undescribed public neoepitopes and confirmed 9 previously reported public neoepitopes.[18 19] Among these positive identifications of public neoepitopes, we described multiple epitopes from genes involved in early carcinogenesis, like p53 mutations, but also for the first time public neoepitopes from resistance-mediating mutations, for example, from the common ESR1 D538G variant which evolves after antihormonal therapy in breast cancer.[20] Thus, our study lays the groundwork for future TCR-based or vaccination studies by providing high-confidence immunotherapy targets. Importantly, the perfect agreement of our positive hits

A

	Clinical response	No response
Not detected	9	32
Detected	2	10
P Value	>0.9999	

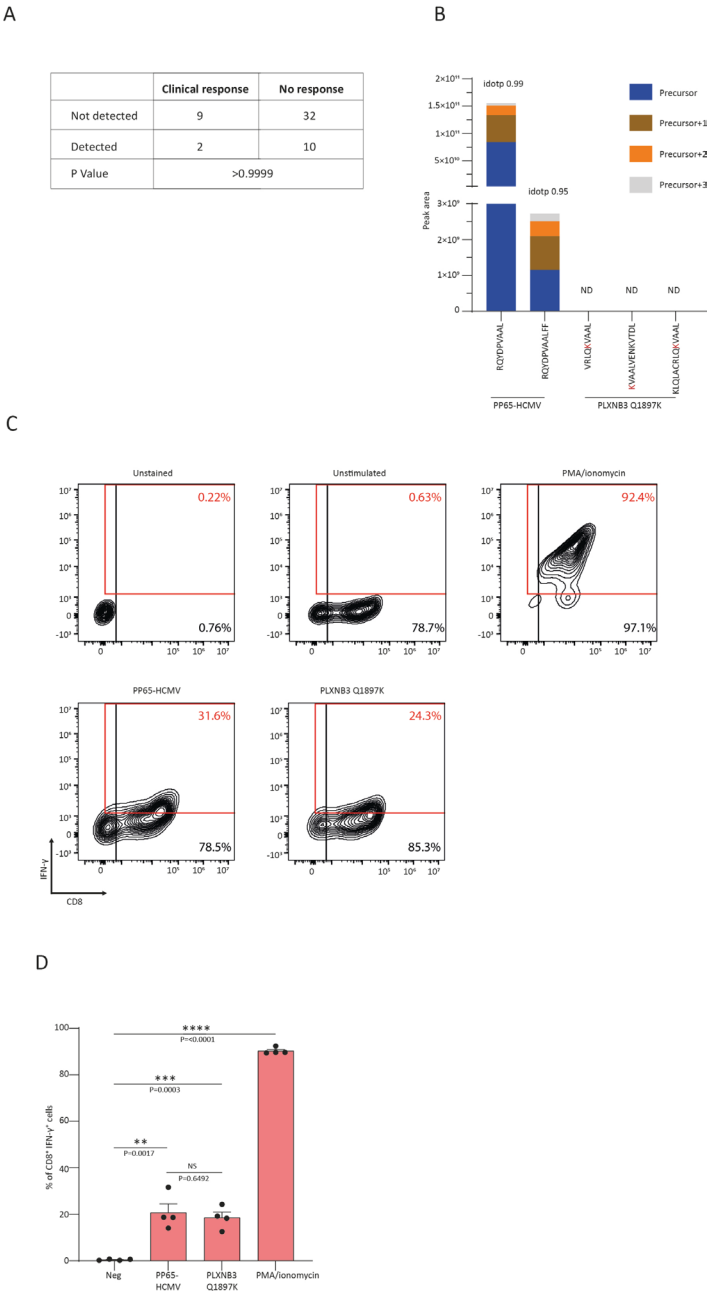

Figure 3 Correlation of private neoepitope presentation and clinically observed T-cell responses. (A) Correlation of reported positive T-cell responses (clinical response) and negative clinical T-cell response (no response) with presentation status (detected and non-detected) of private neoantigens used in this study. Fisher's exact test was used to assess the correlation between clinical T-cell response and neoepitope detection. (B) Bar diagram indicating the peak area (signal in MS measurement) of HLA-bound peptides; here referred to as precursors. Peptides were isolated from COS-7 cells co-transfected with either HLA-A*32:01/PP65 (left) or HLA-A*32:01/PLXNB3 Q1897K (right). Expected peptides are depicted on the X-axis. "+1", "+2", and "+3" indicate isotopic variants of the same peptide. The idotp-values indicate how well the observed distribution of isotopes aligns with the predicted distribution of isotopes. Idotp values above 0.9 are considered correct identifications with one being a perfect score. ND indicates not detected. (C) Representative contour plots showing intracellular IFN-γ expression in HCMV-primed T cells from an HLA-A*32:01 positive healthy donor. T cells were initially stimulated with autologous dendritic cells loaded with HCMV pp65-derived peptide RQYDPVAAL. Primed T cells were incubated with dendritic cells loaded either with the HCMV pp65 peptide or the mutated PLXNB3 Q1897K derived peptide KLQLACRLQKVAAL. Unstained co-cultures and co-cultures of $CD8^+$ T cells with unpulsed DCs (unstimulated) served as negative controls. An additional positive control included T cells primed and stimulated non-specifically with PMA/ionomycin. (D) Bar graphs quantifying the percentage of $CD8^+$/IFN-γ^+ double-positive cells from both donors included in this experiment, each as a replicate, as determined by applying the red gating strategy shown in panel C. An unpaired Student's t-test was performed; mean values±SEM are shown. Each dot represents an individual sample. *p<0.05, **p<0.01, ***p<0.001, ****p<0.0001. DC, dendritic cell; HLA, human leukocyte antigen; HCMV, human cytomegalovirus: IFN, interferon; NS, MS, mass spectrometry; NS, not significant: PMA, Phorbol 12-myristate 13-acetate.

with data published from overexpression experiments in human cells as well as a small subset of results confirmed in K562 cells underlines that even if a monkey antigen processing machinery was used our data are highly comparable.[18 19]

In contrast to our positive hits, 78% of public neoepitopes that were predicted and potentially associated with HLA-LOH were not presented. In consequence, it becomes less likely that the observed HLA-LOH in the suggested HLA contexts is mediated by these mutations. In these patients other public or private neoantigens or tumor-associated antigens presented on the respective HLA allele could be responsible for the observed HLA-LOH.

As many studies on neoantigen target selection and biomarker development for immune checkpoint blockade rely heavily on prediction algorithms,[3 21] our results call for better integration of immunopeptidome data into these approaches as current neoepitope predictions might not provide a solid foundation for biological interpretation of downstream effects of neoantigen presentation. Furthermore, T-cell in vitro assays can lead to positive results independent of the actual target presentation if peptide pulsing or tandem minigenes are used, which both do not resemble processing and presentation of full-length antigens.[22] This was well illustrated when we examined the correlation of neoantigen presentation with clinical T-cell response assessment in an mRNA neoantigen vaccination study in pancreatic cancer.[7] We found no significant correlation between neoepitope presentation and reported T-cell responses, including several examples of observed T-cell responses without sufficient presentation of the putative epitope. This included a predicted HLA-B*07 restricted epitope from the KRAS G12V neoantigen which now in three independent studies has been demonstrated not to be processed and presented, thus corroborating our findings. Even for an HLA-A*32 restricted private neoepitope (from PLXNB3) against which several presumably mutation-specific TCRs were isolated, the minigene used as mRNA vaccine did not generate any neoepitopes in the context of HLA-A*32:01. In contrast, an A*32:01 restricted HLA ligand derived from the CMV pp65 antigen with identical N-terminal amino acid sequence compared with the PLXNB3 sequence was shown to be successfully processed and presented. Additionally, we demonstrated cross-reactivity of HLA-A*32-restricted healthy T cells primed with the pp65 peptide sequence with the mutated PLXNB3 sequence in vitro, which limits the significance of our finding. Therefore, these results cannot ultimately prove that T-cell responses against mutated PLXNB3 are driven by a CMV-specific T-cell clone because the originally isolated TCRs from clinical studies were not available for specificity testing.

In summary, our data highlight the need to critically test prediction results for neoepitopes as conclusions drawn from these datasets without confirmation of presentation might carry so far underestimated biases. This challenges existing neoantigen datasets and has significant implications not only for cancer immunology but also for broader cell biology fields, including autoimmunity and infectious diseases, where prediction tools are widely used. In contrast, positive data like the 24 newly identified public neoepitopes form a strong basis for developing new treatment strategies including immunotherapies against resistance-associated mutations. Our findings suggest that personalized vaccination strategies might benefit from the systematic evaluation of target presentation during the selection process and that whenever possible immunopeptidome experiment should accompany neoepitope-based studies to better understand their underlying biology.

MATERIALS AND METHODS

Cell lines

The monkey fibroblast COS-7 cell line (RRID:CVCL_Z935) was acquired and authenticated through the Leibniz Institute DSMZ-German Collection of Microorganisms and Cell Cultures GmbH (DSMZ accession number ACC 60). K562 cells (RRID:CVCL_0004) were a kind gift from Antonia Busse at Charité. These cells were cultured and maintained in Roswell Park Memorial Institute (RPMI) 1640 medium (Gibco) supplemented with penicillin-streptomycin (Pen-Strep, Gibco) and 10% fetal bovine serum (FBS, GeminiBio). Cells were regularly checked for *Mycoplasm* contamination.

Plasmids

Gene sequences for driver genes and HLA alleles used in our research were synthesized and inserted into the pcDNA3.1+ vector by GenScript. We generated constructs encoding full-length driver genes (except for CTNBB1, which could not be produced in full in our vector) and the HLA alleles of interest. To prepare the RNA for in vitro transcription, we first linearized the plasmid vectors with the Xbal restriction enzyme (New England Biolabs). The linearized plasmids were then purified using the QIAquick PCR Purification Kit (Qiagen) as per the manufacturer's guidelines. In the next step, we synthesized the in vitro RNA from the purified linearized plasmids using the HiScribe T7 High Yield RNA Synthesis Kit (New England Biolabs), following the protocol provided by the manufacturer.

Immunopurification of HLA class I ligands

COS-7 cells were co-electroporated with 100µg/mL of mRNA encoding an individual HLA allele along with the driver protein using the Neon Transfection system (10 µL tip, 1050 V/30 ms/2 pulses). For K562 cells, electroporation was performed using the Neon Transfection system with the 100 µL tip and optimized conditions of 1,000 V, 50 ms, and a single pulse. Approximately 10×10^6 cells were electroporated per condition and subsequently plated in 6-well non-tissue culture-treated plates for overnight incubation. The cells were then harvested by incubation with 1 mM EDTA (Millipore Sigma) at 37°C

for 5 min, followed by pelleting and a single wash in ice-cold RPMI medium (Gibco) and three washes in ice-cold phosphate-buffered saline (PBS) (Gibco). The cells were lysed in 8 mL of 1% CHAPS (Millipore Sigma) for 1 hour at 4°C, after which the lysates were centrifuged at 20,000 g for 1 hour at 4°C, and the supernatant was collected. For the immunopurification of HLA-I ligands, 0.5 mg of W6/32 antibody (Bio X Cell) was conjugated to 40 mg of CN Br-activated sepharose (Cytiva) and incubated with the protein lysate overnight. HLA complexes along with binding peptides were then eluted five times using 1% trifluoroacetic acid (TFA). These peptides and HLA-I complexes were separated using C18 columns (Sep-Pak C18 1 cc Vac Cartridge, 50 mg sorbent, 37–55 µm particle size, Waters), which were pre-conditioned with 80% Acetonitrile (ACN) (Millipore Sigma) and equilibrated with three washes of 0.1% TFA. Samples were loaded onto the columns two times, washed two times with 0.1% TFA, and then eluted in 200 µL of sequentially increased ACN concentrations—15%, 30%, 40%, and 50% in 0.1% TFA. The four fractions were combined, dried using vacuum centrifugation, and stored at −80°C until further processing.

Solid-phase extractions

In-house C18 minicolumns were prepared using the following method: for the solid-phase extraction of a single sample, two small disks (1 mm diameter each) of C18 material were punched out from CDS Empore C18 disks (Thermo Fisher Scientific). These disks were then placed at the bottom of a 200 µL Axygen pipette tip (Thermo Fisher Scientific). The columns were initially washed with 100 µL of 80% ACN in 0.1% TFA and subsequently equilibrated three times with 100 µL of 1% TFA. Fluids were passed through the column by centrifugation in a mini tabletop centrifuge, and the eluates were collected in Eppendorf tubes. Dried samples were then resuspended in 100 µL of 1% TFA, loaded onto the columns, washed two times with 100 µL of 1% TFA, and then run dry. Finally, the samples were eluted with 60 µL of 60% ACN/0.1% TFA, and the resulting sample volume was further reduced by vacuum centrifugation.

Liquid chromatography-tandem mass spectrometry analysis

Samples were analyzed using high-resolution and high-accuracy liquid chromatography-tandem MS on a Vanquish Neo ultra-high-performance liquid chromatography system coupled to an Orbitrap Exploris 480 mass spectrometer (Thermo Fisher Scientific). Peptides were separated on an in-house packed C18 analytical column with a 75 µm inner diameter, 20 cm length, and 1.9 µm beads (Dr Maisch Reprosil-Pur C18-AQ). The chromatographic gradient was applied at a flow rate of 250 nL/min, starting with 2% buffer B, which consisted of 90% acetonitrile and 0.1% formic acid, and 98% buffer A, which consisted of 3% acetonitrile and 0.1% formic acid. Over the first minute, the gradient increased to 5% buffer B, followed by a linear increase to 20% buffer B over the next 34 min. Subsequently, the gradient reached 30% buffer B over a 10 min period and further increased to 60% buffer B over the next 3 min. The system was then washed at 90% buffer B for 6 min before re-equilibration to 2% buffer B. MS was operated in data-dependent acquisition mode with a cycle time of 1 s. Full MS1 spectra were acquired at a resolution of 60,000 in a mass range of 300–1,600. Precursor ions were isolated with a window of 1.2 m/z and fragmented using a normalized collision energy of 28%. MS2 spectra were acquired at a resolution of 30,000 with an automatic gain control target of 100% and a maximum injection time of 150 ms. The dynamic exclusion time was set to 30 s and the intensity threshold specified to 10,000. Only precursor ions with charge states ranging from +1 to +5 were selected for fragmentation.

MS data processing

MS data were processed using Byonic software (V.2.7.84, Protein Metrics) and Peaks software (V.11, Bioinformatics Solutions) on a custom-built server equipped with 4 Intel Xeon E5-4620 8-core CPUs at 2.2 GHz and 512 GB of RAM (Exxact Corporation). The mass accuracy was set to 6 ppm for MS1 and 20 ppm for MS2. Digestion was specified as unspecific, allowing only precursors with charges of +1, +2, and +3 and a maximum mass of 2 kDa. Protein false discovery rate (FDR) was turned off to allow complete assessment of potential peptide identifications. Variable modifications included methionine oxidation; phosphorylation of serine, threonine, and tyrosine; and N-terminal acetylation. Samples were analyzed against a database containing UniProt Cercopithecus aethiops reviewed proteins, supplemented with human mutant sequences of driver genes used in the study and common contaminants. Peptides ranging from 8 to 15 amino acids in length were selected with a minimum log probability value of 1.3, corresponding to p values of 0.05, and duplicates were removed. Ion intensities were exported from Byonic and Peaks for mirror plots. For peak area and retention time analysis, Skyline software (V.24.1, MacCoss Lab Software) was used. Precursor masses of target peptide sequences were searched in all relevant raw files, and peak areas were compared. Retention times for the best-scoring matches were determined using a total of four isotopes.

Assignment of peptide sequences to HLA alleles

To assign peptides that passed the MS quality filters to their most likely HLA complexes, we employed the NetMHCpan 4.1 algorithm (DTU Health Tech) with its default settings. Peptides with an affinity percentage rank below 2 were classified as binders.

Flow cytometry analysis

For the surface HLA staining procedure, approximately 2×10^5 cells in 200 µL of medium were transferred into a 96-well V-bottom plate. The cells were centrifuged at 1,400 rpm for 5 min and then stained with 50 µL of a primary antibody specific to the surface molecule of

interest, diluted in staining buffer (PBS/3% BSA/0.01% NaN_3), for 15 min at 4°C in the dark. Following two washing steps with staining buffer, the samples were resuspended in staining buffer and transferred to tubes for analysis using a Beckman Coulter flow cytometer. For intracellular protein staining, approximately 2×10^5 cells were fixed and permeabilized according to the BD Cytofix/Cytoperm Fixation/Permeabilization Kit protocol (BD Biosciences). The cells were then stained with 50 µL of a primary antibody specific to the intracellular molecule of interest, diluted in Perm/Wash buffer (BD Biosciences), for 15 min at 4°C. After two washing steps with Perm/Wash buffer, the cells were incubated with a fluorescently labeled secondary antibody that targets the isotype of the primary antibody for 15 min at 4°C in the dark. Finally, the samples were washed again, resuspended in staining buffer, and transferred to tubes for acquisition using a Beckman Coulter flow cytometer.

In vitro stimulation of healthy donor PBMCs

Peripheral blood mononuclear cells (PBMCs) from the HLA:A32:01+donor were plated on tissue culture flasks at 1×10^6 cells per cm^2 in complete RPMI media in the absence of cytokine for 2 hours at 37°C to separate the adherent (monocyte-containing) and non-adherent (containing CD8+T cell) fractions. CD8+T cells were then enriched from the non-adherent fraction by untouched negative selection (Miltenyi Biotec). To generate monocyte-derived dendritic cells (moDCs), the adherent fraction was washed with PBS and fresh complete media supplemented with recombinant human interleukin (IL)-4 and granulocyte macrophage colony stimulating factor (GM-CSF) at a concentration of 400 IU/mL were given every alternate day. MoDCs were pulsed by culturing them in RPMI containing 10 µg/mL of synthetic HCMV pp65 peptide RQYDPVAAL, PLXNB3 Q1897K peptide KLQLACRLQKVAAL, for 16–24 hours before transfection and then stimulated with lipopolysaccharide (LPS) (Sigma-Aldrich) and IFN-γ. For priming, healthy donor HLA:A32:01+CD8+T cells were co-cultured with HCMV-pulsed moDCs at an effector-to-target (E:T) ratio of 3:1 in the presence of IL-21 (30 ng/mL) in 24-well non-tissue culture plates (Falcon). Thereafter, the HCMV-primed CD8+T cells were co-cultured with PLXNB3 Q1897K-pulsed moDCs at the same E:T ratio. Wells were replenished with fresh media supplemented with IL-7 and IL-15 at 10 ng/mL every 3 days of the in vitro culture period. All the cytokines used in this experiment were purchased from PeproTech.

T-cell immunoassays

Candidate TCR specificity was assessed by intracellular cytokine staining using the BD Cytofix/CytoPerm Plus Kit, following the manufacturer's instructions. Autologous moDCs from an HLA-A32:01+donor were pulsed by plating them in RPMI containing 10 µg/mL of synthetic peptides HCMV pp65 RQYDPVAAL, or PLXNB3 Q1897K KLQLACRLQKVAAL in 24-well round-bottom plates for 3 hours. Peptides were synthesized by GenScript through individual peptide synthesis. Candidate T cells were co-cultured at an E:T ratio of 3:1 for 16 hours in the presence of Golgi block. PMA-ionomycin unspecific stimulation was included in all experiments as a positive control. Cells were washed in 1×PBS and surface-labeled with anti-CD8-APC-H7 (Clone SK1, Invitrogen) for 30 min at 4°C. Cells were washed with 1×PBS and then fixed and permeabilized for 15 min at 4°C. Surface-labeled cells were then washed with 1×perm wash buffer and labeled with anti-IFN-γ-APC (BD) for 30 min at 4°C in perm-wash buffer. All antibodies were used at a final concentration of 5 µg/mL. Finally, cells were washed with perm-wash buffer, suspended in 2% FBS in PBS, and acquired on an X20 LSRFortessa flow cytometer with BD FACSDiva software. Data were analyzed using FlowJo software V.10.8.1.

Statistics

All graphs except heatmaps were drawn with GraphPad Prism V.10 software. Appropriate statistical tests were used to analyze data, as described in each figure legend. Statistical analyses were performed with GraphPad Prism V.10 software. Significance was preset at $p<0.05$.

Author affiliations
[1]Department of Hematology, Oncology and Tumor Immunology, Hindenburgdamm 30, 12203 Berlin, Germany, Charité – Universitätsmedizin Berlin, corporate member of Freie Universität Berlin and Humboldt Universität zu Berlin, Berlin, BE, Germany
[2]Max Delbruck Centre for Molecular Medicine in the Helmholtz Association, Berlin, Germany
[3]Foundation Medicine Inc, Cambridge, Massachusetts, USA
[4]Berlin Institute of Health at Charite, Berlin, BE, Germany
[5]German Center for Translational Cancer Research (DKTK), DKFZ, Heidelberg, Germany

Acknowledgements We thank Chris Klebanoff, David Scheinberg and Tao Dao for constructive feedback on the manuscript.

Contributors Conceptualization: MM, LAA, PM, MGK. Methodology: BKQZ, ZS, DG, SM, NSL, JS, OP, MH. Investigation: BKQZ, ZS, OP, MH. Visualization: BKQZ. Funding acquisition: MGK. Project administration: MGK. Supervision: MGK. Writing—original draft: BKQZ, MGK. Writing—review and editing: BKQZ, MM, LAA, MGK. MGK is the guarantor.

Funding The study was supported by the Else-Kröner-Fresenius Foundation (2022_EKEA.57)

Competing interests MK works as a consultant for Ardigen P.A., T-Knife GmbH and BioCopy GmbH. MM and LA are employees of Foundation Medicine, Inc. and stockholders of Roche Holding AG.

Patient consent for publication Not applicable.

Ethics approval Only healthy blood donors were included in this study. Written consent was obtained, and the study was approved by the Charité Ethikkomission (EA04/010/25). Participants gave informed consent to participate in the study before taking part.

Provenance and peer review Not commissioned; externally peer reviewed.

Data availability statement Data are available upon reasonable request. Peptide identifications are included in the supplementary files. Mass spectrometry RAW files are available upon request.

ORCID iDs
Badeel Kh Q Zaghla https://orcid.org/0009-0002-2675-8859
Zuhal Safyürek https://orcid.org/0009-0004-8412-5069
Martin G Klatt https://orcid.org/0000-0001-8703-7305

REFERENCES

1 D'Angelo SP, Araujo DM, Abdul Razak AR, *et al*. Afamitresgene autoleucel for advanced synovial sarcoma and myxoid round cell liposarcoma (SPEARHEAD-1): an international, open-label, phase 2 trial. *The Lancet* 2024;403:1460–71.
2 Nathan P, Hassel JC, Rutkowski P, *et al*. Overall Survival Benefit with Tebentafusp in Metastatic Uveal Melanoma. *N Engl J Med* 2021;385:1196–206.
3 Łuksza M, Riaz N, Makarov V, *et al*. A neoantigen fitness model predicts tumour response to checkpoint blockade immunotherapy. *Nature New Biol* 2017;551:517–20.
4 Montesion M, Murugesan K, Jin DX, *et al*. Somatic HLA Class I Loss Is a Widespread Mechanism of Immune Evasion Which Refines the Use of Tumor Mutational Burden as a Biomarker of Checkpoint Inhibitor Response. *Cancer Discov* 2021;11:282–92.
5 Chowell D, Krishna C, Pierini F, *et al*. Evolutionary divergence of HLA class I genotype impacts efficacy of cancer immunotherapy. *Nat Med* 2019;25:1715–20.
6 Sahin U, Derhovanessian E, Miller M, *et al*. Personalized RNA mutanome vaccines mobilize poly-specific therapeutic immunity against cancer. *Nature New Biol* 2017;547:222–6.
7 Rojas LA, Sethna Z, Soares KC, *et al*. Personalized RNA neoantigen vaccines stimulate T cells in pancreatic cancer. *Nature New Biol* 2023;618:144–50.
8 Ott PA, Hu Z, Keskin DB, *et al*. An immunogenic personal neoantigen vaccine for patients with melanoma. *Nature New Biol* 2017;547:217–21.
9 Vitiello A, Zanetti M. Neoantigen prediction and the need for validation. *Nat Biotechnol* 2017;35:815–7.
10 Yewdell JW. MHC Class I Immunopeptidome: Past, Present, and Future. *Mol Cell Proteomics* 2022;21.
11 Shapiro IE, Bassani-Sternberg M. The impact of immunopeptidomics: From basic research to clinical implementation. *Semin Immunol* 2023;66:101727.
12 Wang Q, Douglass J, Hwang MS, *et al*. Direct Detection and Quantification of Neoantigens. *Cancer Immunol Res* 2019;7:1748–54.
13 Chandran SS, Ma J, Klatt MG, *et al*. Immunogenicity and therapeutic targeting of a public neoantigen derived from mutated PIK3CA. *Nat Med* 2022;28:946–57.
14 Klatt MG, Aretz ZEH, Curcio M, *et al*. An input-controlled model system for identification of MHC bound peptides enabling laboratory comparisons of immunopeptidome experiments. *J Proteomics* 2020;228.
15 Klatt MG, Mack KN, Bai Y, *et al*. Solving an MHC allele-specific bias in the reported immunopeptidome. *JCI Insight* 2020;5.
16 Lo W, Parkhurst M, Robbins PF, *et al*. Immunologic Recognition of a Shared p53 Mutated Neoantigen in a Patient with Metastatic Colorectal Cancer. *Cancer Immunol Res* 2019;7:534–43.
17 Hsiue EH-C, Wright KM, Douglass J, *et al*. Targeting a neoantigen derived from a common *TP53* mutation. *Science* 2021;371:eabc8697.
18 Gurung HR, Heidersbach AJ, Darwish M, *et al*. Systematic discovery of neoepitope-HLA pairs for neoantigens shared among patients and tumor types. *Nat Biotechnol* 2024;42:1107–17.
19 Choi J, Goulding SP, Conn BP, *et al*. Systematic discovery and validation of T cell targets directed against oncogenic KRAS mutations. *Cell Rep Methods* 2021;1.
20 Razavi P, Chang MT, Xu G, *et al*. The Genomic Landscape of Endocrine-Resistant Advanced Breast Cancers. *Cancer Cell* 2018;34:427–38.
21 Liu D, Schilling B, Liu D, *et al*. Integrative molecular and clinical modeling of clinical outcomes to PD1 blockade in patients with metastatic melanoma. *Nat Med* 2019;25:1916–27.
22 Immisch L, Papafotiou G, Popp O, *et al*. H3.3K27M mutation is not a suitable target for immunotherapy in HLA-A2^{+} patients with diffuse midline glioma. *J Immunother Cancer* 2022;10.